PCCP

Accepted Manuscript

ROYAL SOCIETY OF CHEMISTRY

www.rsc.org/pccp

Journal Name

RSCPublishing

ARTICLE

Adsorption structures of non-aromatic hydrocarbons on silicalite-1 using single-crystal X-ray diffraction method

Cite this: DOI: 10.1039/xoxxoooooox

Received ooth January 2012,
Accepted ooth January 2012

DOI: 10.1039/xoxxoooooox

www.rsc.org/

Shinjiro Fujiyama,*[a] Shintaro Seino,[a] Natsumi Kamiya,[a] Koji Nishi,[a] Kenji Yoza[b] and Yoshinobu Yokomori[a],

The actual adsorption structures of non-aromatic hydrocarbons on the MFI-type zeolites have not yet been determined. This is due to the presence of twinning, which makes crystallographic analysis difficult. We recently overcame this problem[1], and now report the various adsorption structures of *n*-butane, *n*-pentane, *n*-hexane, 1-butene, *cis* and *trans*-2-butene, 2-butyne and isopentane on silicalite-1 (MFI-type zeolite) as determined via single-crystal X-ray diffraction. The structures were elucidated for both low and high loadings of each guest molecule in order to clarify the adsorption process. The low-loaded structures provide valuable insight into guest-framework interactions and initial adsorption behavior. The *n*-alkanes are initially adsorbed in the sinusoidal channel, while 2-butyne is adsorbed in the straight channel. In the case of the normal hydrocarbons, the molecular configuration (bent or linear) of the compound determines which channel is the preferred adsorption site. Bent molecules prefer the sinusoidal channel and linear molecules prefer the straight channel. In contrast, isopentane is initially adsorbed at the intersection, since the channels are too narrow to maintain the preferred distance between the framework and the bulky isopentane molecule. In the high-loaded structures, the guest molecules occupy additional sites, such that the normal hydrocarbons are located in both channels and isopentane is found at the intersection and the sinusoidal channel.

1. Introduction

Zeolites are promising microporous materials due to their high thermal, mechanical and chemical stability and, for this reason, various applications in catalysis, gas separation and gas storage have been suggested for these substances. Guest molecules in the zeolite micropores are physisorbed in a stable manner even at room temperature, mainly due to van der Waals interactions with the pore walls. MFI-type zeolites such as ZSM-5 and silicalite-1 have in particular attracted a significant amount of interest since they possess two kinds of unique channels. Figure 1 shows the channel system of MFI-type zeolites, which can be divided into three types of sorption sites: straight channel, sinusoidal channel and intersection. The locations of guest molecules are vital to understanding the adsorption properties of the material and this factor has received much attention in recent years. There are a number of reports on adsorption of various hydrocarbons on MFI-type zeolites[2-9] and associated thermodynamic information such as sorption isotherms, heat of sorption and variation of entropy are well established. However, there is currently no consensus concerning the localization of hydrocarbons in the three-dimensional channel network. Jacobs *et al.*[2] has suggested that C_3-C_5 *n*-alkanes do not occupy particular sites while C_6-C_8 *n*-alkanes fill up the straight channel, and that packing in the sinusoidal channel is less dense. Richards *et al.*[3] proposed a sorption model in which a function of sorbate loading describes the measured heat of sorption. They assumed *n*-alkanes are preferentially located in the channels and C_4-C_6 *n*-alkanes are located in the sinusoidal rather than straight channel. Eder *et al.*[6] determined that *n*-alkanes are located in the sinusoidal channel and can also populate the intersection at low loadings. These reports provided valuable thermodynamic data which are useful in terms of understanding the adsorption properties. However, it would be impossible to derive precise locations of guest molecules solely from the thermodynamic data. Computational studies have also been conducted.[10-14] June *et al.*[10,12] concluded that *n*-butane and *n*-hexane are absorbed in both channels in roughly equal proportions, and branched alkanes such as 2- and 3-methylpentane are absorbed at the intersection. Smit *et al.*[13] agree that the probabilities of the C_4-C_6 *n*-alkanes locating in both channels are nearly equal. Maginn *et al.*[14] showed that *n*-butane and *n*-hexane are most likely found in the sinusoidal channel, while Titiloye *et al.*[11] reported that adsorption in the straight channel is preferred in the case of C_1-C_8 *n*-alkanes.

Localization of these hydrocarbons by computational studies, however, has not yet been conclusive.

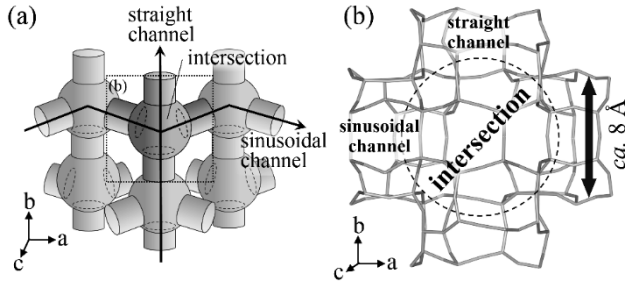

Fig. 1 The channel system of MFI-type zeolite (MFI): (a) a schematic illustration of the pore topology and (b) the intersection-centered framework with adjoining channels.

In the present study we experimentally determined the adsorption structures of both normal and branched C_4-C_6 hydrocarbons in MFI-type zeolites using single-crystal X-ray diffraction (XRD). Silicalite-1 (Al free MFI-type zeolite) was selected as adsorbents to leave the cationic sites in the framework out of discussion. The structures of silicalite-1 loaded with various hydrocarbons provide valuable insight about the van der Waals interaction, which is the dominant interaction between guest molecules and micropore. While, the H-bonding with isolated silanol species of crystal defects has somewhat possibilities. [15-18] The structures were determined at low and high loadings for each guest molecule to clarify the adsorption process. The low-loaded structures directly indicate the most preferred sorption sites based on guest-framework interactions since the loadings are too low for guest-guest interactions to affect the locations of the guest molecules. The high-loaded structures show the locations of guest molecules occupying additional sites, which are the second and third most stable sorption sites. The low- and high-loaded structures of each guest hydrocarbons reveal the adsorption process of the hydrocarbons.

Many structures consisting of MFI-type zeolites loaded with aromatic compounds have been determined using single-crystal XRD.[19-26] However, there are no reports concerning the locations of non-aromatic hydrocarbons, despite the heightened interest in this subject. These structures have not yet been determined due to the twinning problem, which makes the crystallographic analysis highly challenging. MFI-type zeolites such as ZSM-5 and silicalite-1 have twinned monoclinic phases except when bulky aromatic compounds are present in their pore structures.[26] Recently, we have overcome this problem by applying mechanical stress along the *c* axis at high temperatures and using a refinement for pseudo-merohedral twinning.[1] This paper therefore represents the first-ever report describing the adsorption structures of non-aromatic hydrocarbons on silicalite-1.

2. Experimental

2.1 Preparation of silicalite-1 single crystals loaded with hydrocarbons

Silicalite-1 single crystals were synthesized according to a method described by Kamiya *et al.*[26,27] EDX analysis confirmed that the obtained crystals consisted of SiO_2 with no Al or cation species present. Crystals selected for X-ray structural analysis were pressed by applying a mass of 2.0 g along the crystallographic *c* axis, while raising the temperature from ambient to 473 K and cooling back to ambient. This heating and cooling cycle was repeated three times for each specimen.[26] The crystals were subsequently exposed to the hydrocarbons at 298 K in a closed apparatus (BV-001 bell jar-type vacuum oven, Sibata Scientific Technology, Ltd. or BELSORP-max, BEL Japan, Inc.). The experiment was conducted carefully not to let the samples be exposed to humid atmosphere in order to exclude the effects of water molecules in the pore on the adsorption behaviors.[28,29] The experimental conditions applied to each sample are summarized in Table 1.

Table 1 Adsorption conditions for each sample at 298 K.

Guest	low-loaded		high-loaded	
	pressure (kPa)	time (h)	pressure (kPa)	time (h)
n-butane	90	3	90	70
n-pentane	*ca.* 70[a]	2	*ca.* 70[a]	6
n-hexane	*ca.* 20[a]	24	*ca.* 20[a]	96
1-butene	20	1	90	36
cis-2-butene	20	1	90	96
trans-2-butene	20	1	90	96
2-butyne	20	3	20	168
isopentane	*ca.* 90[a]	48	*ca.* 90[a]	168

[a] saturated vapor pressure

2.2 Single-crystal XRD analysis

Single-crystal X-ray diffraction data were collected at room temperature in air using an APEX II, APEX II Ultra or D8 VENTURE (Bruker AXS) with Mo Kα radiation. The collected reflections were corrected for Lorentz polarization and the absorption effect. The structural analysis was conducted in the monoclinic twin in $P2_1/n$. The structure was solved using the direct method, and difference-Fourier synthesis was applied to the remaining atoms (SHELXTL[30]). The pseudo-merohedral twinning refinement was performed on F^2 and $\Sigma w||F_o|-|F_c||^2$ was minimized based on $w = 1/[\sigma^2(F_o^2)+(aP)^2 + bP]$, where $P = (F_o^2 + 2F_c^2)/3$ and *a* and *b* are the weighting parameters. The refinement as twin was done by introducing the command line "TWIN" with the twin law (-100 010 00-1) to transform the *hkl* indices of one phase into the other phase. The reciprocal lattices of the twin phases can be treated as coincident due to the similarity of their c^* axes (a^* and b^* are common). As a result, almost all reflections are overlapped and the pseudo-merohedral twinning refinement proceeds successfully.[1] The refinement of the framework atoms was converged with no restraints, after which refinement with the guest hydrocarbons was conducted. A difference-Fourier map clearly showed electron density peaks in the pores and these peaks were added to the calculations as carbon atoms. The structures of hydrocarbons with no degree of freedom of C-C bond rotation (*cis* and *trans*-2-butene and 2-butyne) were constrained to act as rigid structures, while the bond lengths associated with 1, 2

and 1, 3 distances were restrained in the other hydrocarbons. As an example, the 1, 2 and 1, 3 distances of the saturated alkanes were constrained at 1.53 and 2.54 Å, respectively. As a final step, the structures incorporating the guest hydrocarbons were successfully solved. Anisotropic displacement parameters were used for the framework atoms and isotropic parameters were used for the hydrocarbons. The crystal data and refinement details are summarized in Table 2, and the full details are available as CIF files in Supplementary Information. The structures in Figs. 2 to 4 and 7 to 9 were generated using the VESTA software package.[31]

Table 2 Crystal data and refinement details.

Crystal	*n*-butane		*n*-pentane	
	low-loaded	high-loaded	low-loaded	high-loaded
Chemical formula[a]	$Si_{24}O_{48}\cdot0.9C_4$	$Si_{24}O_{48}\cdot2.0C_4$	$Si_{24}O_{48}\cdot1.0C_5$	$Si_{24}O_{48}\cdot2.0C_5$
Crystal size (mm^3)	0.17 × 0.09 × 0.07	0.23 × 0.11 × 0.07	0.16 × 0.07 × 0.04	0.13 × 0.09 × 0.05
Independent reflections (R_{int})	13290 (0.148)	12710 (0.144)	12993 (0.147)	13092 (0.110)
No. of restraints	5[c]	15[c]	7[c]	21[c]
No. of parameters	667	701	671	713
R_1 ($I > 2\sigma(I)$), R_{all}	0.0555 (6076[b]), 0.1646	0.0506 (6752[b]), 0.1245	0.0594 (6408[b]), 0.1623	0.0492 (5585[b]), 0.1371
$\Delta\rho_{max}$ and $\Delta\rho_{min}$ (e $Å^{-3}$)	1.15 and -0.79	0.64 and -0.82	1.05 and -0.61	0.62 and -0.57
Crystal	*n*-hexane		1-butene	
	low-loaded	high-loaded	low-loaded	high-loaded
Chemical formula[a]	$Si_{24}O_{48}\cdot0.7C_6$	$Si_{24}O_{48}\cdot2.0C_6$	$Si_{24}O_{48}\cdot1.1C_4$	$Si_{24}O_{48}\cdot2.0C_4$
Crystal size (mm^3)	0.26 × 0.13 × 0.07	0.18 × 0.10 × 0.07	0.16 × 0.10 × 0.05	0.15 × 0.12 × 0.08
Independent reflections (R_{int})	12034 (0.089)	12094 (0.152)	13278 (0.170)	13341 (0.103)
No. of restraints	9[c]	43[c, d]	10[c]	15[c]
No. of parameters	675	722	684	698
R_1 ($I > 2\sigma(I)$), R_{all}	0.0416 (10366[b]), 0.0501	0.0455 (9106[b]), 0.0593	0.0525 (4054[b]), 0.1963	0.0498 (5700[b]), 0.1345
$\Delta\rho_{max}$ and $\Delta\rho_{min}$ (e $Å^{-3}$)	0.96 and -0.55	0.81 and -0.68	0.64 and -0.57	0.54 and -0.50
Crystal	*cis*-2-butene		*trans*-2-butene	
	low-loaded	high-loaded	low-loaded	high-loaded
Chemical formula[a]	$Si_{24}O_{48}\cdot0.8C_4$	$Si_{24}O_{48}\cdot1.1C_4$	$Si_{24}O_{48}\cdot1.1C_4$	$Si_{24}O_{48}\cdot1.9C_4$
Crystal size (mm^3)	0.17 × 0.11 × 0.08	0.16 × 0.10 × 0.06	0.14 × 0.09 × 0.07	0.17 × 0.13 × 0.08
Independent reflections (R_{int})	13037 (0.081)	13365 (0.085)	13015 (0.084)	12984 (0.064)
No. of restraints	0	0	0	0
No. of parameters	666	676	666	674
R_1 ($I > 2\sigma(I)$), R_{all}	0.0484 (5784[b]), 0.1217	0.0486 (5411[b]), 0.1353	0.0513 (5390[b]), 0.1332	0.0464 (6609[b]), 0.1043
$\Delta\rho_{max}$ and $\Delta\rho_{min}$ (e $Å^{-3}$)	0.88 and -0.49	0.86 and -0.57	0.92 and -0.47	0.92 and -0.44
Crystal	2-butyne		isopentane	
	low-loaded	high-loaded	low-loaded	high-loaded
Chemical formula[a]	$Si_{24}O_{48}\cdot0.2C_4$	$Si_{24}O_{48}\cdot1.8C_4$	$Si_{24}O_{48}\cdot0.3C_5$	$Si_{24}O_{48}\cdot2.0C_5$
Crystal size (mm^3)	0.23 × 0.11 × 0.06	0.16 × 0.09 × 0.05	0.17 × 0.12 × 0.07	0.21 × 0.11 × 0.07
Independent reflections (R_{int})	12810 (0.094)	12818 (0.132)	12864 (0.106)	13020 (0.107)
No. of restraints	0	15[d, e]	8[c]	16[c]
No. of parameters	661	676	671	692
R_1 ($I > 2\sigma(I)$), R_{all}	0.0534 (6505[b]), 0.1164	0.0550 (5423[b]), 0.1506	0.0549 (6589[b]), 0.1203	0.0520 (5815[b]), 0.1269
$\Delta\rho_{max}$ and $\Delta\rho_{min}$ (e $Å^{-3}$)	0.58 and -0.60	0.69 and -0.68	0.55 and -0.60	0.90 and -0.57

[a] 1.0 guest molecule for an asymmetric unit of framework ($Si_{24}O_{48}$) corresponds to a loading of 4.0 molecules per unit cell. The unit cell consists of 4 asymmetric units in $P2_1/n$.
[b] No. of reflections with $I > 2\sigma(I)$
[c] restraints on the bond lengths of the guest hydrocarbons.
[d] restraints on the displacement parameters of the guest hydrocarbons.
[e] restraints on the occupancy factors of the guest hydrocarbons.

3. Results and Discussion

3.1 Adsorption of *n*-alkanes

Figure 2 shows the low-loaded *n*-alkane-silicalite-1 structures. All alkanes are located in the centers of the sinusoidal channels, which are determined to be the most stable sorption sites. The occupancy factors, which are all equal to or close to 1.0, indicate that the sinusoidal channels are almost fully occupied. The *n*-alkanes are never observed at other sites, such as the straight channel and intersection. The sinusoidal channel thus represents a significantly stable sorption site for the *n*-alkanes. The distances between neighboring *n*-alkanes, defined as the internuclear distances between closest carbon atoms, are 6.46, 5.21 and 3.91 Å respectively for *n*-butane, *n*-pentane and *n*-hexane. This distance decreases with increasing chain length and thus end-to-end guest-guest interactions will be particularly enhanced in the case of *n*-hexane.

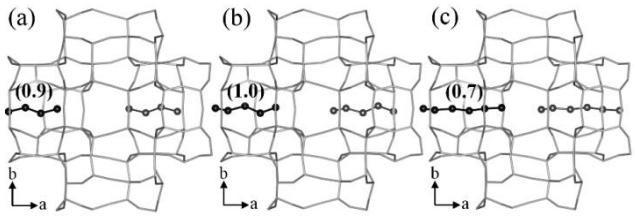

Fig. 2 Low-loaded structures of (a) *n*-butane, (b) *n*-pentane and (c) *n*-hexane with the occupancy factors shown in parentheses. The locations related to the 2_1 screw axis along the *a* axis are shown in gray.

Fig. 3 presents the high-loaded structures determined for the *n*-alkane-silicalite-1. The *n*-alkanes are located in the both channels. The occupancy factors indicate the loadings consist of eight molecules per unit cell, which is approximately equal to the adsorption capacities of normal C_4-C_6 alkanes.[2,3,7] The fully-packed structures corresponding to the sorption of these *n*-alkanes were determined. The distances between guest *n*-alkanes are listed in Table 3. There exists considerable guest-guest dispersion interaction in these high-loaded structures, based on the short intermolecular distances. With the exception of the SIN to STR1 *n*-hexane interaction, these compounds interact in end-to-end structures.

The adsorption process of the *n*-alkanes is revealed by these results. These compounds are initially adsorbed in the sinusoidal channels, due to favorable guest-framework interactions, until the sinusoidal channels are fully occupied at four molecules per unit cell. The guest-guest interactions are weak in this initial stage, although they are enhanced in the case of *n*-hexane. Additional guest molecules are adsorbed in the straight channel and guest-guest interactions subsequently arise. Finally, both channels are fully occupied, at eight molecules per unit cell. This process is in good agreement with the packing model proposed by Richards *et al.*[3] The model was derived from the heats of sorption associated with various levels of loading. The end-to-end guest-guest interactions of *n*-hexane in the low-loaded structure at a distance of 3.91 Å clearly explain the rapid increase in the heat of sorption over the loading range of zero to four molecules per unit cell, with an increase of 20 kJ/mol.[3] Even at low loading levels, *n*-hexane molecules in the sinusoidal channels strongly interact with one another. A moderate increase in the heat of sorption over the same low loading range is also observed in case of *n*-butane (about 5 kJ/mol).[3] This increase is caused by the interactions between *n*-butane in the sinusoidal channel and *n*-butane at the other locations such as straight channel or intersection, even though *n*-butane molecules were not observed in the single XRD measurements in the present study, since the associated occupancy levels were too low. *n*-Pentane also shows an increase in heat of sorption in the low loading range, on the order of 18 kJ/mol.[5] In addition to interactions with *n*-pentane at the other locations (as seen in the case of *n*-butane), this change in heat of sorption may also result from the end-to-end guest-guest interactions of *n*-pentane in the sinusoidal channels at a distance of 5.21 Å.

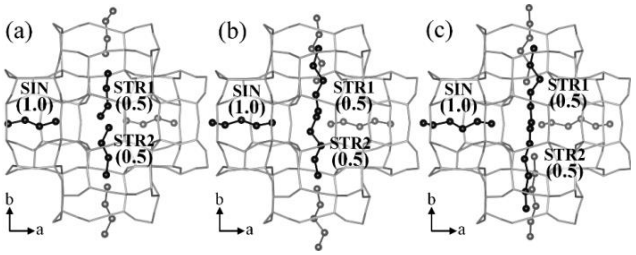

Fig. 3 High-loaded structures of (a) *n*-butane, (b) *n*-pentane and (c) *n*-hexane with the occupancy factors shown in parentheses. The locations related to the 2_1 screw axis along the *a* axis and the center of symmetry in the middle of the straight channel are shown in gray.

Table 3 Internuclear distances (Å) between the closest carbon atoms of neighboring *n*-alkanes in the high-loaded structures.

	n-butane	*n*-pentane	*n*-hexane
SIN – STR1	3.91	4.49	3.97[a]
SIN – STR2	4.44	3.35	3.44
STR1 – STR2	6.18	3.18	2.94

[a] end atom of SIN to second atom from the end of STR1.

3.2 Adsorption of 2-butyne

Figure 4(a) shows the low-loaded structure of 2-butyne-silicalite-1, in which the 2-butyne is located in the straight channel. The guest-guest interactions in this structure are negligibly small since the 2-butyne molecules are located separately. The shortest distance between neighboring 2-butyne molecules is 10 Å, which is too far to allow guest-guest interactions. The structure clearly indicates that the straight channel is the most stable sorption site based on the guest-framework interactions. The molecular configuration (bent or linear) determines which channel is the most stable site based on guest-framework interactions. Bent molecules prefer the sinusoidal channel and linear molecules prefer the straight channel. Indeed, the bent dimethyl ether is initially adsorbed in the sinusoidal channel[32] while the linear CO_2 is initially adsorbed in the straight channel.[33] These results may be explained by the structural differences between the channels.

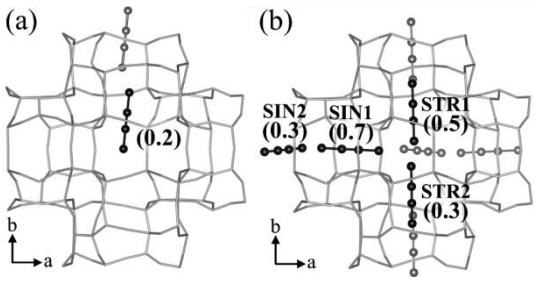

Fig. 4 (a) Low-loaded structure and (b) high-loaded structure of 2-butyne with the occupancy factors shown in parentheses. The locations related to the 2_1 screw axis along the *a* axis and the center of symmetry in the middle of the straight channel are shown in gray.

Simple calculations of the Lennard-Jones potential are useful as a means of estimating the stability of sorption sites based on channel structures and guest molecule configurations. The potential between an imaginary atom at an arbitrary

position and the framework oxygen atoms around the channels can be calculated using the well-known Equation (1).

$$U(x,y,z) = 4\varepsilon \sum_i \{(\sigma/r_i)^{12} - (\sigma/r_i)^6\} \quad (1)$$

Here (x, y, z) represents the arbitrary position of the imaginary atom, r_i is the distance between the atom and the framework oxygen atom i, σ is the separation at which the potential becomes zero, and ε is the depth of the potential well. The van der Waals radius of the imaginary atom is set at 1.7 Å in accordance with the radii of common atoms such as carbon, nitrogen and oxygen. The 426 framework oxygen atoms around the channels are counted in the calculation (i = 1 ~ 426). The details of the calculation has been reported elsewhere.[32] The potential map of the resulting $U(x, y, z)$ values reflects the structural differences of the channels and a guest molecule at a stable sorption site will locate its atoms where $U(x, y, z)$ is low. Fig. 5 shows the locations of the most stable sorption sites of various guest molecules with the Lennard-Jones potential maps. The potential is normalized to cancel an unknown factor 4ε. As can be seen in Figs. 5(a) and (c), there are deep potential wells in both channels. The depths of which are approximately the same with a difference of less than 2%. This is not unexpected, since the pore sizes are roughly the same. However, the configuration of the potential wells is clearly different in the two cases. Based on the minimum potential paths indicated by the dashed lines, the path of the sinusoidal channel is winding while that of the straight channel is linear. So the sinusoidal channel is more favorable for bent molecules and the straight channel is more favorable for linear molecules. The bent *n*-butane is located within the winding minimum path and the linear 2-butyne molecules are found along the linear minimum path. Figs. 5(b) and (d) indicate the locations of the most stable sorption sites for dimethyl ether[32] and CO_2.[33] These locations are almost identical to those determined for *n*-butane and 2-butyne, as expected, since the locations are determined simply on the basis of van der Waals interactions. As a result, the locations at which the interaction potentials are minimized should be similar.

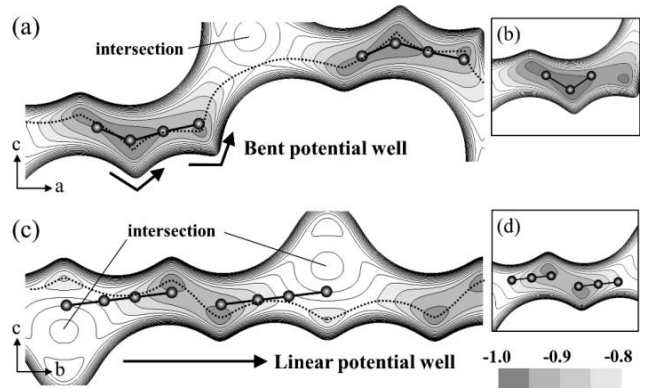

Fig. 5 Locations of the most stable sorption sites for guest molecules with the normalized Lennard-Jones potential maps: (a) *n*-butane in the sinusoidal channel, (b) dimethyl ether in the sinusoidal channel,[32] (c) 2-butyne in the straight channel and (d) CO_2 in the straight channel.[33] The contour lines represent values ranging from -0.95 to 0.00 in increments of 0.05. The potential minimum paths are indicated by dashed lines.

Fig. 4(b) shows the high-loaded structure of 2-butyne-silicalite-1. The internuclear distances between the closest carbon atoms of neighboring 2-butyne molecules are 2.91 and 3.09 Å for the SIN1 to STR2 and SIN1 to STR1 locations, respectively. Guest-guest interactions are at work in this structure. The occupancy factors indicate that the level of loading is 7.2 molecules per unit cell, which is comparable to the reported saturation loading at 298 K of 9.40 molecules per unit cell.[4] The small difference between these values is due to the extra sorption sites, which are highly disordered. These sorption sites are much less stable and the associated occupancy factors are too low to be observed on the basis of XRD. Unlike the *n*-alkanes, the 2-butyne located in the sinusoidal channel is in a state of disorder. This occurs because the potential well in the sinusoidal channel is winding and the linear configurations of the 2-butyne molecules prevent them from locating within the winding well. As shown in Fig. 6, 2-butyne is located on the linear part of the winding well.

The adsorption process of 2-butyne is similar to those of the *n*-alkanes except for the initial sorption site. The 2-butyne molecules are initially adsorbed in the straight channel due to guest-framework interactions, while additional molecules are adsorbed in the sinusoidal channel, leading to guest-guest interactions. Finally, the both channels are almost fully occupied (7.2 molecules per unit cell).

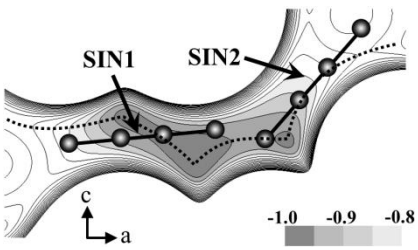

Fig. 6 SIN1, 2 of the high-loaded 2-butyne-silicalite-1 in the sinusoidal cannel, with the normalized Lennard-Jones potential map. The contour lines represent values ranging from -0.95 to 0.00 in increments of 0.05. The potential minimum paths are indicated by dashed lines.

3.3 Adsorption of 1-butene and *cis* and *trans*-2-butene

Figure. 7 shows the low-loaded structures of 1-butene and *cis* and *trans*-2-butene. These molecules are located in both channels even at low loadings of about four molecules per unit cell, indicating that the sorption stabilities of the channels are similar. The initial adsorption behavior is intermediate between those of the bent *n*-alkanes and the linear 2-butyne. Thus the molecular configuration (bent or linear) or, in other words, the bond angles within the guest molecule, is an important factor that determines which channel is the most stable sorption site for normal hydrocarbons. As the bond angles approach 180°, the compounds exhibit a greater tendency to prefer the straight channel. Fig. 8 shows the high-loaded structures of 1-butene and *cis* and *trans*-2-butene, in which the guest molecules are

located in the both channels, in common with the other normal hydrocarbons. The 1-butene and *cis* and *trans*-2-butene adsorption processes are therefore the same as those of the normal hydrocarbons, except for the initial adsorption behavior. The concerted adsorption on both channels proceeds initially in case of 1-butene and *cis* and *trans*-2-butene.

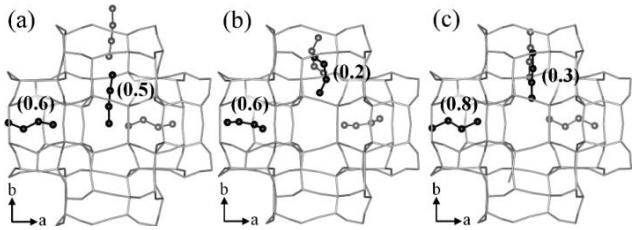

Fig. 7 Low-loaded structures of (a) 1-butene, (b) *cis*-2-butene and (c) *trans*-2-butene with the occupancy factors shown in parentheses. The locations related to the 2_1 screw axis along the *a* axis and the center of symmetry in the middle of the straight channel are shown in gray.

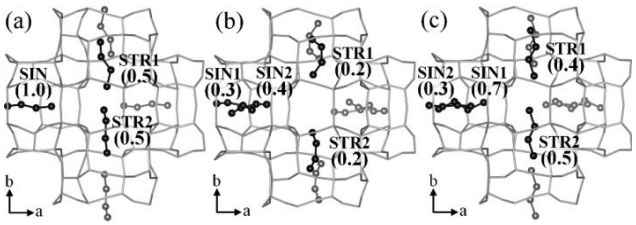

Fig. 8 High-loaded structures of (a) 1-butene, (b) *cis*-2-butene and (c) *trans*-2-butene with the occupancy factors shown in parentheses. The locations related to the 2_1 screw axis along the *a* axis and the center of symmetry in the middle of the straight channel are shown in gray.

3.4 Adsorption of isopentane

Figure 9(a) shows the low-loaded structure of isopentane-silicalite-1. The guest-guest interactions are negligibly small because the isopentane molecules are located separately. The structure indicates that the intersection is the most stable sorption site based on the guest-framework interactions. Unlike the normal hydrocarbons, that show a preference for the channels as sorption sites, isopentane is initially adsorbed at the intersection, since the pore size of the intersection is larger than those of the channels. The shortest distances between carbon atoms of guest hydrocarbons and framework atoms in the low-loaded structures are listed in Table 4. The framework atoms here are all oxygen. The values are all in the vicinity of 3.6 Å, which is the distance allowing the hydrocarbons to minimize the van der Waals interaction potentials. Isopentane is relatively bulky due to its branched structure, and thus the channels are too narrow to allow the isopentane molecules to maintain the appropriate distance. Isopentane is thus initially adsorbed at the large intersection so as to keep the appropriate distance and to minimize the interaction potentials. Bulky aromatic compounds are also adsorbed at the intersection at low loadings.[19-21] The correlation between the bulkiness of guest molecules and the pore size of the initial sorption site is discussed in a previous report[33] based on the integrated Lennard-Jones potential model.[34]

Table 4 Shortest internuclear distances (Å) between carbon atoms of guest hydrocarbons and framework atoms (all oxygen) in the low-loaded structures.

Guest	Location	Distance
n-butane	sinusoidal channel	3.754
n-pentane		3.654
n-hexane		3.715
1-butene	both channels	3.500 (SIN), 3.854(STR)
cis-2-butene		3.296 (SIN), 3.689(STR)
trans-2-butene		3.506 (SIN), 3.516(STR)
2-butyne	straight channel	3.785
isopentane	intersection	3.675

Fig. 9(b) shows the high-loaded structure of isopentane-silicalite-1. The occupancy factors indicate the loading in this structure is eight molecules per unit cell, which is approximately equal to the adsorption capacity of isopentane.[2] The fully-packed structure of isopentane was determined. The associated internuclear distance between the nearest carbon atoms of the INT and SIN locations is 3.07 Å. Guest-guest dispersion interactions are assumed, considering the short intermolecular distance. The orientation of the INT molecules in the high-loaded structure is different from that of the low-loaded structure due to these guest-guest interactions. Fig. 10 shows the SIN of the high-loaded isopentane-silicalite-1 with the normalized Lennard-Jones potential map. As previously discussed, bulky molecules such as isopentane generally disfavor the narrow channels. However, the relatively wide potential well of the sinusoidal channel allows isopentane to locate itself within the area of the potential well. The sinusoidal channel then acts as the second most stable site.

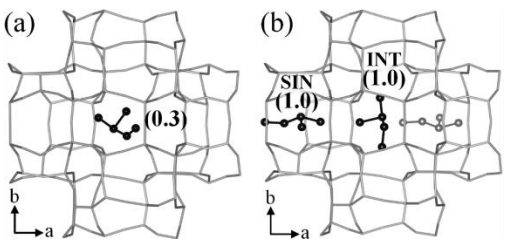

Fig. 9 (a) Low-loaded structure and (b) high-loaded structure of isopentane with the occupancy factors shown in parentheses. The location related to the 2_1 screw axis along the *a* axis is shown in gray.

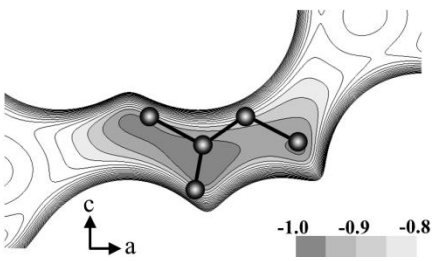

Fig. 10 SIN of the high-loaded isopentane-silicalite-1 in the sinusoidal channel, with the normalized Lennard-Jones potential map. The contour lines range from -0.95 to 0.00 in increments of 0.05.

Millot *et al.*[9] noted that isopentane might prefer the intersections, using a temperature-programmed-equilibration

method, and June *et al.*[10] has suggested that the initial sorption site of 2- and 3-methylpentane is the intersection, based on molecular simulations. They predicted the locations of the branched alkanes with high precision.

4. Conclusions

The adsorption structures of various hydrocarbons were experimentally determined using single-crystal X-ray diffraction. It was found that, based on guest-framework interactions, normal hydrocarbons prefer the narrow channels while the bulky isopentane prefers the large intersections. Moreover, the configuration of the normal hydrocarbons (bent or linear) is an important factor in determining which channel is the stable sorption site; bent molecules prefer the sinusoidal channel and linear molecules prefer the straight channel. The adsorption processes for these compounds were also revealed. The bent *n*-alkanes are initially adsorbed in the sinusoidal channel and later are adsorbed in both channels, although the linear 2-butyne molecules are initially adsorbed in the straight channel and are later adsorbed in both channels. Isopentane is initially adsorbed at the large intersection and is subsequently located at the intersection and in the sinusoidal channel.

Notes and references

[a] National Defense Academy of Japan, Yokosuka, Japan.
[b] Bruker AXS, Yokohama, Japan.

Electronic Supplementary Information (ESI) available: Crystallographic data (CIF formatted files). See DOI: 10.1039/b000000x/

1 S. Fujiyama, N. Kamiya, K. Nishi and Y. Yokomori, *Z. Kristallogr.*, 2014, **229**, 303.
2 P. A. Jacobs, H. K. Beyer and J. Valyon, *Zeolites*, 1981, **1**, 161.
3 R. E. Richards and L. V. C. Rees, *Langmuir*, 1987, **3**, 335.
4 D. Shen and L. V. C. Rees, *Zeolites*, 1991, **11**, 684.
5 M. S. Sun, O. Talu and D. B. Shah, *J. Phys. Chem.*, 1996, **100**, 17276.
6 F. Eder and J. A. Lercher, *Zeolites*, 1997, **18**, 75.
7 B. Millot, A. Methivier and H. Jobic, *J. Phys. Chem. B*, 1998, **102**, 3210.
8 M. S. Sun, D. B. Shah, H. H. Xu and O. Talu, *J. Phys. Chem. B*, 1998, **102**, 1466.
9 B. Millot, A. Méthivier, H. Jobic, I. Clemençon and B. Rebours, *Langmuir*, 1999, **15**, 2534.
10 R. L. June, A. T. Bell and D. N. Theodorou, *J. Phys. Chem.*, 1990, **94**, 1508.
11 J. O. Titiloye, S. C. Parker, F. S. Stone and C. R. A. Catlow, *J. Phys. Chem.*, 1991, **95**, 4038.
12 R. L. June, A. T. Bell and D. N. Theodorou, *J. Phys. Chem.*, 1992, **96**, 1051.
13 B. Smit and J. I. Siepmann, *J. Phys. Chem.*, 1994, **98**, 8442.
14 E. J. Maginn, A. T. Bell and D. N. Theodorou, *J. Phys. Chem.*, 1995, **99**, 2057.
15 I. Braschi, G. Gatti, G. Paul, C. E. Gessa, M. Cossi and L. Marchese, *Langmuir*, 2010, **26**, 9524.
16 R. Arletti, A. Martucci, A. Alberti, L. Pasti, M. Nassi and R. Bagatin, *J. Solid State Chem.*, 2012, **194**, 135.
17 A. Martucci, L. Pasti, M. Nassi, A. Alberti, R. Arletti, R. Bagatin, R. Vignola and R. Sticca, *Micropor. Mesopor. Mater.*, 2012, **151**, 358.
18 V. Sacchetto, G. Gatti, G. Paul, I. Braschi, G. Berlier, M. Cossi, L. Marchese, R. Bagatin and C. Bisio, *Phys. Chem. Chem. Phys.*, 2013, **15**, 13275.
19 H. van Koningsveld, J. C. Jansen and A. J. M. de Man, *Acta Cryst.*, 1996, **B52**, 131.
20 H. van Koningsveld and J. C. Jansen, *Micropor. Mater.*, 1996, **6**, 159.
21 H. van Koningsveld and J. H. Koegler, *Micropor. Mater.*, 1997, **9**, 71.
22 H. van Koningsveld, F. Tuinstra, H. van Bekkum and J. C. Jansen, *Acta Cryst.*, 1989, **B45**, 423.
23 H. van Koningsveld, J. C. Jansen and H. van Bekkum, *Acta Cryst.*, 1996, **B52**, 140.
24 K. Nishi, A. Hidaka and Y. Yokomori, *Acta Cryst.*, 2005, **B61**, 160.
25 N. Kamiya, T. Oshiro, S. Tan, K. Nishi and Y. Yokomori, *Micropor. Mesopor. Mater.*, 2013, **169**, 168.
26 N. Kamiya, W. Iwama, T. Kudo, T. Nasuno, S. Fujiyama, K. Nishi and Y. Yokomori, *Acta Cryst.*, 2011, **B67**, 508.
27 N. Kamiya, Y. Torii, M. Sasaki, K. Nishi and Y. Yokomori, *Z. Kristallogr.*, 2007, **222**, 551.
28 J. Farrell, C. Manspeaker and J. Luo, *Micropor. Mesopor. Mater.*, 2003, **59**, 205.
29 L. Pasti, A. Martucci, M. Nassi, A. Cavazzini, A. Alberti and R. Bagatin, *Micropor. Mesopor. Mater.*, 2012, **160**, 182.
30 G. M. Sheldrick, *Acta Cryst.*, 2008, **A64**, 112.
31 K. Momma and F. Izumi, *J. Appl. Cryst.*, 2011, **44**, 1272.
32 S. Fujiyama, S. Seino, N. Kamiya, K. Nishi and Y. Yokomori, *Acta Cryst.*, submitted.
33 S. Fujiyama, N. Kamiya, K. Nishi and Y. Yokomori, *Langmuir*, 2014, **30**, 3749.
34 G. J. Tjatjopoulos, D. L. Feke and J. A. Mann, Jr., *J. Phys. Chem.*, 1988, **92**, 4006.

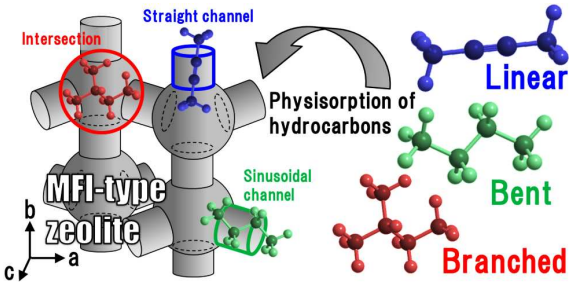

The adsorption structures of the various hydrocarbons on silicalite-1 are revealed experimentally using single-crystal X-ray method.